DNA-modified silicon nanocrystals studied by X-ray luminescence and X-ray absorption spectroscopies: Observation of a strong infra-red luminescence band

P. R. Coxon, M. Newman, M. R. C. Hunt, N. O'Farrell, B. R. Horrocks, N. R. J. Poolton, and L. Šiller

Citation: Journal of Applied Physics **111**, 054311 (2012); doi: 10.1063/1.3691600
View online: https://doi.org/10.1063/1.3691600
View Table of Contents: http://aip.scitation.org/toc/jap/111/5
Published by the American Institute of Physics

DNA-modified silicon nanocrystals studied by X-ray luminescence and X-ray absorption spectroscopies: Observation of a strong infra-red luminescence band

P. R. Coxon,[1,a)] M. Newman,[2] M. R. C. Hunt,[2] N. O'Farrell,[3] B. R. Horrocks,[3] N. R. J. Poolton,[1,4] and L. Šiller[1,a)]
[1]*School of Chemical Engineering and Advanced Materials, Newcastle University, Newcastle upon Tyne, NE1 7RU, United Kingdom*
[2]*Department of Physics, Durham University, South Road, Durham, DH1 3LE, United Kingdom*
[3]*School of Chemistry, Newcastle University, Newcastle upon Tyne, NE1 7RU, United Kingdom*
[4]*Photon Science Institute, University of Manchester, Manchester M13 9PL, United Kingdom*

(Received 18 November 2010; accepted 2 February 2012; published online 8 March 2012)

Silicon nanocrystals (SiNCs) modified with 18-mer DNA oligonucleotides have been studied by X-ray excited optical luminescence (XEOL) and X-ray absorption spectroscopy (XAS) in photoluminescence yield (PLY) and total electron yield (TEY) modes. Luminescence spectra from the DNA-modified SiNCs under X-ray excitation display distinct differences from simple alkyl terminated SiNCs. The DNA-modified SiNCs show strong luminescence at 540 ± 10 nm under vacuum ultraviolet excitation which is assigned to nitrogen $1s - \sigma^*$ transitions within the DNA bases. Under excitation at 130 eV the PLY spectra from the same samples show the native nanocrystal ultraviolet emission band is suppressed, and the strongest emission peak is red shifted from 430 ± 10 nm to 489 ± 10 nm which we attribute to base nitrogen $1s$ transitions. In addition, a strong emission band in the infrared region at 815 ± 10 nm is observed. This clearly resolved strong IR band from the DNA-modified SiNCs may provide a useful luminescence signature in cell-labeling techniques and open up a range of applications for *in vivo* assays. © *2012 American Institute of Physics*. [http://dx.doi.org/10.1063/1.3691600]

I. INTRODUCTION

DNA has become an increasingly popular subject of study in nanotechnology, for example, there is interest in the use of DNA as a scaffold template to build complex two and three-dimensional nanoscale architectures,[1–3] as a data processor within molecular computing[4,5] or as a potential component in the production of lab-on-a-chip devices and sensors for biological targets.[6,7] Fluorescent DNA markers employing cadmium-based nanocrystals have attracted considerable interest since it was found[8] that capping the CdSe nanoparticle with a ZnS layer resulted in increased room temperature quantum yields. Although the first programed assembly of CdSe DNA-functionalized nanocrystals was reported more than decade ago,[9] the use of cadmium-based nanoparticles within living systems has been questioned owing to the inherent toxicity of the nanocrystal core[10,11] and their propensity to agglomerate within restricted volumes.[12] In response to these concerns, attention has turned toward nanocrystals with less harmful chemistries. Silicon-based nanoparticles have shown themselves to be promising candidates in diagnostic applications as cellular markers because they have greater stability and similar quantum yields when compared with cadmium nanocrystals.[13–15]

Several groups have reported the synthesis of DNA molecules covalently-attached to silicon surfaces through a variety of intermediate linker groups.[16–19] At present the majority of the work carried out upon silicon-based DNA sensing devices has concentrated upon either surface modification of bulk material for sensor platforms through self-assembled monolayers for DNA immobilization,[20] or through hybridization with silicon nanowire arrays.[21] In comparison, the coupling of silicon nanoparticles with biomolecules has been less prevalent largely due to challenges in rendering the nanocrystals water-dispersible and compatible with biological fluid environments. To date only one study has been conducted where, in 2004, Wang and coworkers labeled DNA with amino-functionalized silicon nanocrystals with a view to ascertain their feasibility as fluorescent markers.[22]

Following our development of a synthetic route for fabricating stable, fluorescent alkylated silicon nanocrystals through electrochemical etching,[23] their optical and electronic properties have been investigated in detail.[24–27] Studies have been carried out to test the stability of the nanocrystal luminescence within aqueous solutions over extended durations to assess their survival in cellular environments[15] and to demonstrate their lack of cytotoxicity.[28] Owing to the high surface-to-volume ratio the luminescence is, in principle, sensitive to the surface states. For nanocrystals which are used as biological markers, interaction between the nanocrystal surface and biomolecule may influence the efficiency of electron-hole recombination[29] leading to variations in the emitted light. With this in mind, in order to establish their

[a)]Authors to whom correspondence should be addressed. Electronic addresses: p.r.coxon@ncl.ac.uk and lidija.siller@ncl.ac.uk.

viability as potential biological labels, it is desirable to identify and understand any behavioral changes upon coupling with common biological molecules.

We have previously reported the attachment of DNA to nanocrystalline porous silicon and its characterization.[18] The method we employ, of synthesizing the DNA at nanocrystalline porous silicon, rather than attaching pre-formed DNA strands, has some advantages. In particular, the synthetic procedure via solid-phase methods ensures the absence of DNA molecules not bound to the nanocrystals. The reason is that unbound DNA molecules are automatically washed away during the standard oligosynthesis protocol. The work contained within this paper extends the preparation by disrupting the porous silicon to disperse the DNA-modified nanocrystals in aqueous media and describes the results from photoluminescence and X-ray absorption studies upon silicon nanocrystals coupled to DNA chains. The main aim of this study is to identify changes in the nanoparticle luminescence spectra in response to modification. Luminescence profiles from the DNA modified silicon nanocrystals have been investigated by X-ray excited optical luminescence (XEOL) and optically-detected X-ray absorption spectroscopy (OD-XAS). Characterization by XEOL offers particular advantages over conventional luminescence spectroscopies in nanoscale composite systems owing to its chemical state and site selectivity.[30]

II. EXPERIMENTAL

DNA-nanocrystal samples were synthesized in a two-part process. In the first stage, solid-phase DNA oligomers were grown upon alkylated porous silicon wafers using an automated DNA synthesizer (Expedite 8909 Nucleic Acid Synthesizer, PED Applied Biosystems) analogous to the procedure detailed in Ref. 18. In brief, an organic monolayer is formed on the porous Si which contains a vinyl group at one end to react with the Si-H surface and a hydroxy group at the other on which to synthesize DNA. The link between the Si and the monolayer is an Si-C bond that is extremely resistant to chemical attack, even by aqueous alkali. The link between the DNA and the monolayer is via a C-O bond to a phosphate.[18] The synthesis of DNA at hydrogen-terminated silicon via such monolayers produces DNA molecules which remain anchored even after heating in aqueous solution.[18] A suspension of nanocrystal-DNA structures was formed from the DNA-porous silicon wafers by breaking the chip surfaces with a needle and sonicating the powder in water. That the DNA remains attached to the Si after sonication is verified by the water solubility of Si-DNA nanoparticles (see Supplementary Material[59]) whereas the original alkylated Si nanoparticles are not water soluble in the absence of DNA. It is also worth noting that electrophoresis of the Si-DNA particles shows no evidence of free DNA, which would not be expected for a simple mixture of nanocrystals and DNA.

Nanocrystals formed by the ultrasonic disruption of porous silicon show very similar luminescent characteristics to those formed through thermally-induced mechanical fracture.[23] We have repeated some of the spectroscopic characterization of unmodified SiNCs on the DNA modi fied SiNCs, but we present this data in the supplementary material[59] accompanying this paper because the main conclusion of that work is that the DNA-modified SiNCs have similar Si core size and similar photoluminescence characteristics, at least under visible excitation, to unmodified SiNCs.

The DNA chains bound to the nanocrystal samples (SiNCs-DNA) comprise an 18-mer (polymer units) with a base sequence: 5′ - GCG -TAC -TAT - CAG -TCA - GAT - 3′. The sequence strand was linked to the nanocrystal at the 3′ – end. The sequence used in this work is fully synthetic. Its structure was chosen in order to prevent self-hybridization, which results in a less ordered, kinked structure as the single strand hybridizes and folds back upon itself. In this work SiNCs bearing synthesized single-stranded DNA are termed "DNA-modified" SiNCs. Alkyl terminated SiNCs prepared as described in Ref. 26 we call "unmodified" SiNCs. The same the C_{11} capping monolayer is present on both SiNC surfaces (as shown in the molecular model presented in the supplementary material[59]). The presence of DNA at the surface of the SiNCs has been confirmed by infra-red spectroscopy, Raman spectroscopy, and photoluminescence spectroscopy (see supplementary material[59]). Both preparation methods involve electrochemical etching of bulk silicon wafers, the main difference in preparation is that a lower current density (75 mA cm^{-2} versus 400 mA cm^{-2}) is applied to produce the DNA-modified SiNCs since porous Si layers prepared at higher current densities are not sufficiently stable to survive the multi-step procedures of solid-phase DNA synthesis.

XEOL and OD-XAS measurements were performed using the Mobile Luminescence End-Station (MoLES) (Ref. 31) on Beamline MPW 6.1 at SRS, Daresbury, UK and at Beamline-52, MAX-I, MAXLab Sweden. The DNA-modified SiNCs were re-dispersed in a suspension of dichloromethane (dichloromethane provides a convenient means to transfer the SiNCs as it evaporates rapidly) and placed dropwise onto a clean tantalum foil substrate (Goodfellow, UK) which was mounted on a closed cycle helium cryostat using carbon tape to maintain good electrical and thermal contact. Measurements were made at room temperature and at 10 K. XEOL from DNA-modified SiNCs was studied using vacuum ultraviolet (VUV) photons with an energy of 21.2 eV at Max-Lab (to enable comparison with data taken using laboratory based sources) and soft x-ray photons with an energy of 130 eV (i.e., above the Si $L_{2,3}$ edge) at SRS, Daresbury. In the latter case, the approximate flux at the sample was 10^{12} photons per second, with a spot size of 2.0×0.4 mm^2. The choice of excitation energies permits direct comparison of the DNA-modified SiNC samples with previous XEOL measurements performed upon alkyl-terminated SiNCs prepared by similar methods.[27,32] Wavelength selective luminescence spectra were recorded using a 0.19 m, $f = 3.9$ optical spectrometer (Triax-190, Jobin-Yvon) using three different gratings. Two gratings blazed at 250 nm and 630 nm provided a nominal optical resolution of 6 nm and a spectral range spanning the UV/visible/NIR from 200 to 860 nm (recorded using a multi-alkali photomultiplier tube). A 600 l/mm grating provided a resolution of 12 nm in the near infra-red (NIR) range from 800 to 2000 nm, which was recorded using a cooled Ge

detector. All emission spectra presented here have been corrected for instrumental response.

OD-XAS spectra were collected across the silicon *L*-edge, the carbon *K*-edge and the nitrogen *K*-edge in total electron yield (TEY) and total luminescence yield (TLY) modes. The total electron yield was recorded by the drain current method, while the TLY was obtained with the monochromator set to zero order and detecting over the full bandwidth of the photomultiplier tube (PMT), 200–860 nm; both modes were recorded simultaneously. OD-XAS measured over the nitrogen edge is of particular interest since nitrogen is only expected within nucleobase compounds and so any absorption and/or luminescence signatures in this spectral region will serve as a useful indicator of the presence of DNA. All spectra have been normalized to account for systematic variations in the beamline flux and instrumental response. OD-XAS spectra were normalized to the incident X-ray flux collected by either the luminescence yield from an ultrapure quartz specimen or from the photo-current generated from a gold grid, both sited before the sample. The quartz reference sample was used for normalization over the carbon and nitrogen absorption edges. Spectra over the silicon absorption edge were normalized to the flux measured by the gold grid. Energies were calibrated against the π^* peak of highly oriented pyrolytic graphite (HOPG), located at 285.38 eV.[33]

III. RESULTS AND DISCUSSION

Figure 1 shows the photoluminescence spectra from the unmodified SiNC sample [Fig. 1(a)] and the DNA-modified SiNCs [Fig. 1(b)]. The luminescence intensity is comparable with and without DNA attachment. The vertical line denotes where spectra obtained using the different gratings described above have been spliced together. The spectra were taken at 300 K with a photon energy of 130 eV. At this energy, the *L* shell of both pure silicon and silicon oxide are excited. The spectrum from the unmodified SiNC sample shows three major features: a broad peak at ~420 nm, a broad peak at ~630 nm, and a series of sharper peaks within a band between 210 and 310 nm. The series of sharp peaks for the unmodified SiNCs are likely to arise from the presence of trace amounts of toluene remaining from their synthesis, as has been suggested by Rosso Vasic *et al.*[34] These sharp features are absent from the DNA-modified SiNC sample due to the more rigorous washing procedures employed in the synthesis of this material. The peak at ~420 nm from the unmodified SiNCs [Fig. 1(a)] is the blue emission band which has been previously associated with oxidized Si within the passivating layer at the SiNC surface.[25] If one compares the position of the blue band from the unmodified SiNCs with that of the modified SiNCs [Fig. 1(b)], it is clear that this band is shifted from ~420 nm to ~445 nm. In XEOL and X-ray emission measurements upon silicon nanowires Sham and co-workers have also attributed a blue emission at ~460 nm to a silicon oxide layer.[35] The presence of SiO_x in our DNA-modified SiNCs is confirmed by Fourier-transform infra-red (FTIR) spectroscopy and XAS (see supplementary Material[59]). A significant difference between the preparation of the unmodified SiNCs and DNA-modified SiNCs is the oxidative step involved in transforming phosphorus (III) to phosphorus (V) during DNA synthesis in the latter. Due to the phosphoramidite chemistry specific to DNA synthesis, it very likely that the SiO_x species at the surface of the DNA-modified SiNC differ from those of the unmodified SiNC surface leading to the observed shift of the blue band.

It is notable that the strong emission observed at 630 nm in the unmodified SiNCs associated with orange light emission appears broadened and shifted in the DNA-modified SiNCs (Fig. 1). To investigate this further we undertook XEOL measurements of the nanocrystals under VUV excitation (21.2 eV) and 300 K and 10 K, as shown in Fig. 2.

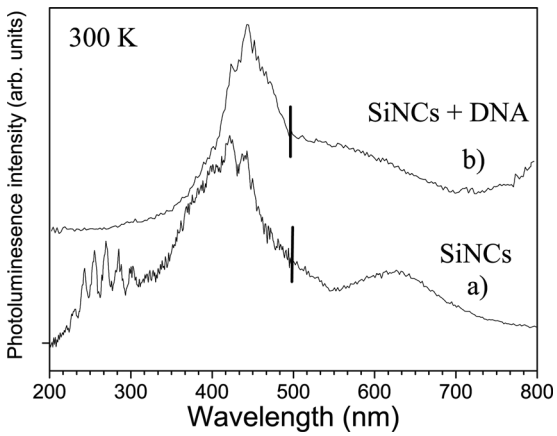

FIG. 1. Photoluminescence spectra from (a) unmodified SiNCs and (b) DNA-modified SiNCs acquired through excitation with 130 eV photons. The sample temperatures were 300 K. The vertical line denotes where two spectra from different gratings has been spliced together.

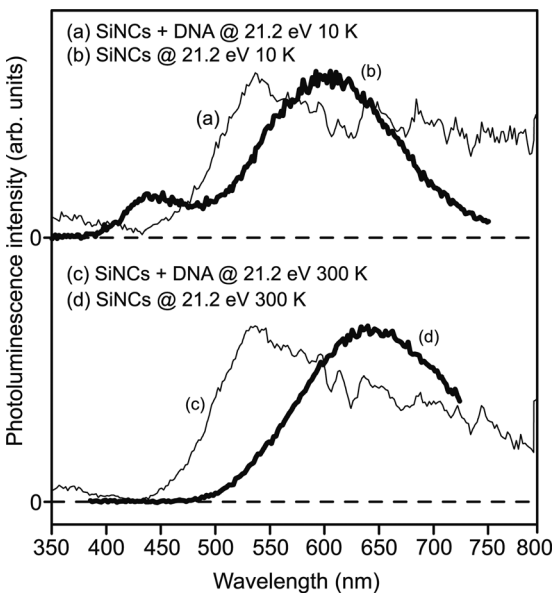

FIG. 2. X-ray excited optical photoluminescence spectra for unmodified SiNCs and the DNA modified SiNCs excited at 21.2 eV measured at 10 K (a) and (b) and at 300 K (c) and (d), respectively. All spectra have been scaled to the same maximum intensity for clarity while the spectra collected at 10 K have been shifted vertically to ease comparison. The dashed lines indicate the zero intensity position.

Again clear differences can be observed between the spectra of the DNA-modified and the unmodified SiNC samples. There is a shift of the emission intensity in the 450–750 nm range to shorter wavelength from the DNA-modified SiNCs compared with the unmodified SiNC sample. Such a blue-shift was not observed when luminescence experiments were performed with Argon ion laser excitation at 488 nm (see supplementary material[59]). This suggests that the observed emission is due to an energy transfer process which requires larger excitation energy. It is notable that the spectra from the DNA-modified SiNC sample show an extended asymmetric profile toward the red end of the spectrum. It can also be seen that in both the spectra from the DNA-modified samples [Figs. 2(a) and 2(c)] the leading edges of the luminescence show much steeper profiles than for the unmodified SiNCs: this form appears independent of sample temperature and can be seen at both 10 K and 300 K.

At first inspection the emission band centered at 540 ± 10 nm in the spectra from the DNA-modified SiNCs might be thought to arise from a shift of the orange emission band observed in the unmodified SiNCs. However, there is a significant dependence on temperature of the position of this emission band from the unmodified SiNCs. The orange band from the unmodified SiNCs is blue shifted from 630 nm to 600 nm as the sample temperature is decreased from 300 K to 10 K [Figs. 2(b) and 2(d)], as we have observed previously.[25] This shift has been suggested to arise from population of localized tail states which are formed by the disordered surface potential arising from variations in the nanocrystal surface stoichiometry and roughness.[25] There is no similar temperature dependence of the emission from the DNA-modified SiNCs which show the same line shape and position at both temperatures, hence this emission feature originates from a different process.

A blueshift of 35.1 nm has been observed in photoluminescence (PL) spectra from HgTe nanocrystals upon coupling with a 22-base single strand of DNA at room temperature.[36] The shift in the narrow PL band was ascribed to changes in the refractive index of the DNA modified system and to saturation of the nanocrystal dangling bonds by the negatively-charged strand wrapping around the nanocrystal. Further work[37] attributed the narrow blue-shifted bands to quantum confinement effects and localization of excitons by a surface dipole layer induced by the different dielectric constants of the DNA and nanocrystal, leading to a shortening of radiative combination lifetimes thus aiding rapid radiative transitions. Although the species in the samples studied in our work have significantly different dielectric constants, ε for double-stranded DNA has been measured as $\sim$80 (Ref. 38) against 11.7 for bulk silicon, reducing further within nanoscale systems,[39] the width of the bands at 530 nm in Figs. 2(a) and 2(c) is too large for excitonic emission and therefore cannot be attributed to localized excitons in this case.

Blue-shifting of nanocrystal emission has also been reported within CdSe-DNA assemblies upon hybridization with biological specimens.[40] The authors suggested the shifts may be caused by energy-transfer processes related to the hybridization between the nanocrystal and the target biostructure or through selective quenching of the native luminescence of the CdSe. Further insight into the nature of the luminescent sites which give rise to the emission at $\sim$540 nm in the DNA-modified SiNCs may be gained by collecting filtered luminescence over the absorption edges of an element of interest. Since nitrogen is present within the bases of the DNA it was decided to scan the excitation energy across the nitrogen absorption threshold while collecting filtered luminescence sampled at 542 nm. Figure 3 shows the partial photon yield (PPY) spectrum obtained at 542 nm emission over the nitrogen *K*-edge at 10 K. A sharp minimum at 405 eV may be clearly observed. The minimum corresponds to an inverted peak due to self-absorption effects arising from the sample thickness.[41] Such inversions are regularly observed in standard XAS measurements using yield techniques, for example photoconductivity XAS studies and X-ray fluorescence spectra.[42] Inversions in the luminescence occur because the sample thickness is far greater than the penetration depths of the photons at the energies specific to the absorption edges (the thick film of DNA-modified SiNCs is estimated to have a thickness of the order of several tens of microns) and as a result all incident light is absorbed by the sample. The position of the feature at 405 eV is in good agreement with the nitrogen absorption profiles of nucleobases and amino acid compounds. Previous absorption studies have shown that all are dominated by a broad absorption around 406 eV which has been attributed to $1s$ - σ^* transitions[43–45] within the nitrogenous bases. Thus the luminescence band at 540 nm can be linked to the presence of nitrogen. From this evidence we suggest that the luminescence observed from the DNA-modified SiNCs centered at 542 nm arises from the DNA itself, rather than from sub-stoichiometric oxides on the silicon nanocrystals. The role of SiO_x can be neglected because SiO_2 emits in a very clear band with a maximum at 440 nm (and extends between 400 and 500 nm), as seen in Fig. 2(b). This emission originates from self-trapped excitons. A reduction of "x" from "2" in SiO_x would lead to a strong red-shift; but equally, the quantum efficiency will rapidly decrease too. Therefore, it is very unlikely that the emission at 542 nm originates from SiO_x on the SiNCs.

Further support for the presence of DNA in intimate contact with the SiNCs in the DNA-modified SiNC sample is

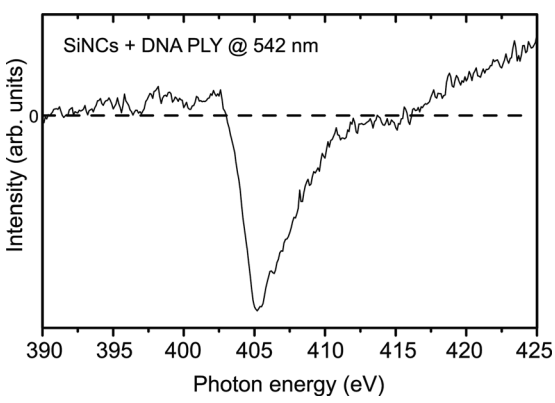

FIG. 3. Partial photoluminescence yield (PPY) spectrum at 542 nm collected over the nitrogen *K*-edge from DNA-modified SiNCs.

provided by XAS across the carbon *K* edge, Fig. 4. OD-XAS spectra from the DNA-modified SiNCs taken at 10 K are shown in Fig. 4(b). The luminescence yield is inverted with respect to the electron yield showing a decrease in intensity as the $1s$ - π^* transition is reached by self-absorption or non-radiative absorption channels, as discussed above. Both the luminescence [Fig. 4(b)] and electron yield [Fig. 4(a)] profiles exhibit generally similar shapes.

Generally XAS profiles of DNA, especially those around the nitrogen and carbon absorption edges, are noticeably influenced by the π^* orbitals in the nucleobases.[46] Stacking interactions and the phosphate backbone have also been shown to play a role in the absorption structure.[47] The high flexibility of the biomolecule also gives rise to the existence of different local configurations of nominally identical moieties, which tends to broaden out the respective spectral features.[48] The samples studied here have a further order of complexity with the inclusion of the alkyl chain linking the oligonucleotide to the nanocrystal surfaces, leading to further disorder.

Although a few studies have been performed upon double and single-stranded multibase DNA chains (typically immobilized upon modified Au substrates),[49,50] the vast majority of experimental and theoretical XAS studies on DNA have limited their concern to single nucleobase, nucleoside or nucleotide samples so as to preserve fine structural features and to aid spectral analysis and identification [for example, Refs. 51–53]. Owing to the differing carbon species within the DNA-nanocrystal sample and differences in local environment resulting from disorder, as discussed above, we are not able to resolve the absorption fine structures characteristic of the individual nucleobases such as those reported in Refs. 45 or 54. However, the TLY spectrum shows a sharp dip at ~284.5 eV which matches with the center of the doublet in the TEY spectrum (shown by the dashed line). In spite of the lack of absorption fine structure, we can attribute this dip to dipole $1s$ - π^* transitions arising from

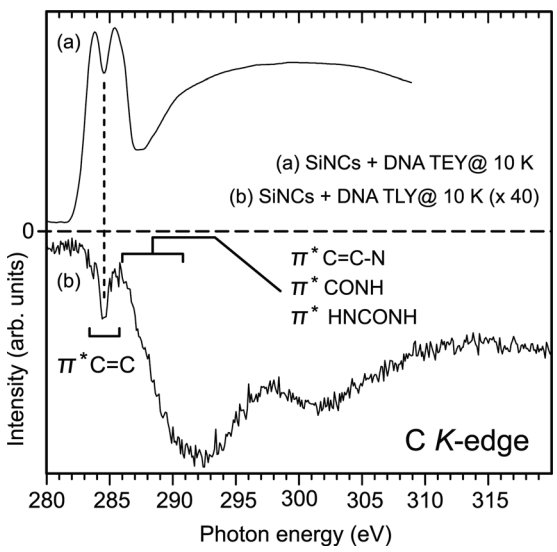

FIG. 4. XAS spectra from DNA-modifed SiNCs acquired over the carbon *K*-edge, in (a) total electron yield (TEY) and (b) total luminescence yield (TLY) yield modes.

within C=C functional groups that are present within all the nucleobases. This assignment agrees with those given to fine resonance absorption peaks lying within the 284 − 285 eV energy range found previously.[45,55] From 286 to 290 eV a broad absorption dip may be observed. This region is labeled π^* C=C-N, π^* CONH, π^* HNCONH following the work of Ref. 45 upon calibrated DNA base reference samples. In addition, a higher energy feature in the TLY at ~301.6 eV is observed which is related to σ^* resonances not involved in luminescence or bonding. Although it is not possible to resolve clear resonance structures, the C=C related signal provides a clear signature which confirms the presence of DNA within the sample.

We can eliminate the possibility that photon-induced degradation of DNA (and any resulting photo-induced reactions at the SiNC surface) has a significant influence on our measured PL and OD-XAS results: It has been shown that a significant buildup of reaction products in DNA due to damage by X-ray photons with a flux density comparable to that used in this work occurs only after approximately 2 h of constant irradiation.[56] This is because the cross-section for DNA degradation by photons in the VUV energy range is almost two orders of magnitude smaller than that for low energy electrons and that the threshold value for photon induced damage is several eV higher than for low-energy electrons (3–20 eV).[57] Since in this work the PL data are acquired within a few minutes and OD-XAS spectra are measured within ~10 min, we believe that for the results presented our measurements are sufficiently rapid that photo-induced DNA damage is minimal.

In addition to the emission at 540 nm the DNA-modified SiNCs also show strong emission intensity compared with the unmodified SiNCs at wavelengths above 700 nm, as can be seen in Figs. 1(b), 2(a), and 2(c). The far infra-red emission from the DNA-modified SiNCs is shown more clearly over the extended wavelength range presented in Fig. 5, which shows the room temperature XEOL spectrum excited with 130 eV photons. There is a clear peak in the emission located at 815 ± 10 nm which has a full width at half maximum (FWHM) of ~250 nm. In our previous work a very weak and narrow emission line located at ~792 nm with a shoulder at 810 nm was observed from unmodified SiNCs (Ref. 27) excited by 150 eV photons (above the oxidized Si absorption edge) but only at low temperature (12 K). This emission was attributed to radiative recombination of valence excitons. However, the peak observed in Fig. 5 is very clear, although broad, even at room temperature. We do not consider this band to be related to the native room temperature emission of bulk silicon which is centered at 1137 nm (Ref. 55) and is therefore some way from the IR band observed in this work. Instead we suggest that the presence of DNA at the surface of the DNA-modified SiNCs can affect PL through, for example, the passivation of surface trap states.[29] Increased radiative recombination would then enable the XEOL signal to be observed even at room temperature and may explain the relatively large width of this peak. An alternative possibility is that if, as a result of the C_{11} alkyl chain, the DNA is too far away from the silicon surface to effectively passivate surface states there could easily be

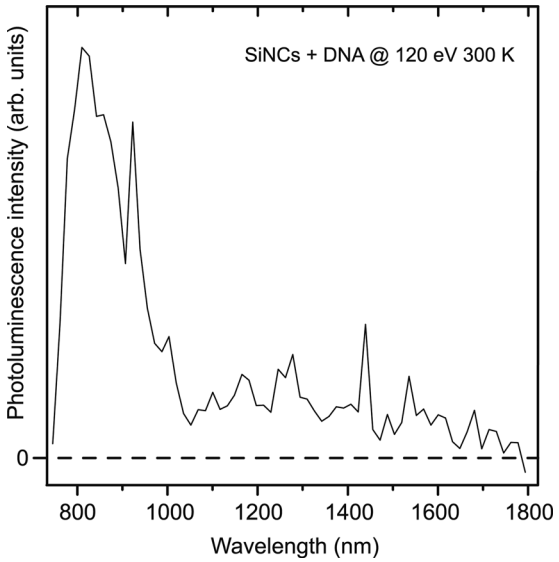

FIG. 5. XEOL spectrum from the DNA-modifed SiNCs over the NIR/IR region. The incident excitation energy and sample temperature is indicated within the figure.

long-range screening effects since ssDNA is a highly charged, flexible polyanion.

The clearly resolved 815 nm IR band observed for DNA-modified SiNCs could provide a useful luminescent signature in cell-labeling techniques and open up a range of applications for *in vivo* assays. Emission toward the red end of the visible spectrum is highly desirable in cellular labels since light in this region is only weakly absorbed by cells in living systems and is well separated from the normal range of cellular emission.[58] Consequently, the use of near-infrared emitting nanocrystals has attracted much interest, especially in deep-tissue imaging studies where they are estimated to increase the sensitivity of tumor imaging by tenfold, which would extend the sensitivity of cancer detection limits down to 10 - 100 cells.

IV. CONCLUSIONS

Silicon nanocrystals covalently bound to short DNA chains have been studied by X-ray excited optical luminescence and X-ray absorption spectroscopies. The DNA modified SiNCs exhibit a shift of the nanocrystal blue photoluminescence band from ~420 nm to ~445 nm when compared to the "unmodified" SiNCs. This redshift is explained in terms of changes to surface oxidation of the SiNCs as a consequence of the preparation procedures. Emission is also observed at 540 nm in the DNA-modified SiNCs which is suggested to arise from the DNA, on the basis of energy filtered OD-XAS performed over the nitrogen *K*-edge. Upon coupling of SiNCs with DNA, a strong emission band in the infrared region at 815 ± 10 nm has been discovered. This is a particularly striking find and one which may open up potential uses of silicon nanocrystals within biological imaging technologies.

ACKNOWLEDGMENTS

The authors gratefully acknowledge the assistance of Dr. A. Pike and Dr. Y. Chao in preparing the samples. P.R.C. is thankful to Newcastle University for award of a studentship. The authors are grateful to Cenamps and EPSRC (Grant No. EP/F065272/1) for financial support.

[1]E. Braun, Y. Eichen, U. Sivan, and G. Ben-Yoseph, Nature **391**, 775 (1998).
[2]J. Richter, M. Mertig, W. Pompe, I. Monch, and H. Schackert, Appl. Phys. Lett. **78**, 536 (2001).
[3]K. Keren, R. S. Berman, E. Buchstab, U. Sivan, and E. Braun, Science **302**, 1380 (2003).
[4]L. Adleman, Science **266**, 1021 (1994).
[5]J. Zhao, Z. Zhang, Y. Shi, X. Li, and L. He, Chin. Sci. Bull. **49**, 17 (2004).
[6]B. Castner and D. Ratner, Surf. Sci. **500**, 28 (2002).
[7]R. C. Somers, M. G. Bawendi, and D. G. Nocera, Chem. Soc. Rev. **36**, 579 (2007).
[8]M. Hines and P. Guyot Sionnest, J. Phys. Chem. **100**, 468 (1996).
[9]G. Mitchell, C. Mirkin, and R. Letsinger, J. Am. Chem. Soc. **121**, 8122 (1999).
[10]A. Shiohara, A. Hoshino, K. Hanaki, K. Suzuki, and K. Yamamoto, Microbiol. Immunol. **48**, 669 (2004).
[11]J. Lovric, H. Bazzi, Y. Cuie, G. Fortin, F. Winnik, and D. Maysinger, J. Mol. Med. **83**, 377 (2005).
[12]M. Akerman, W. Chan, P. Laakonen, S. Bhatia, and E. Ruoslahti, Proc. Natl. Acad. Sci. U.S.A. **99**, 12617 (2002).
[13]D. Jurbergs, E. Rogojina, L. Mangolini, and U. Kortshagen, Appl. Phys. Lett. **88**, 233116 (2006).
[14]G. Belomoin, J. Therrien, A. Smith, S. Rao, R. Twesten, S. Chaieb, M. Nayfeh, L. Wagner, and L. Mitas, Appl. Phys. Lett. **80**, 841 (2002).
[15]F. Dickinson, T. Alsop, N. Al-Sharif, C. Berger, H. Datta, L. Šiller, Y. Chao, E. Tuite, A. Houlton, and BR. Horrocks, Analyst (Cambridge U.K.) **133**, 1573 (2008).
[16]T. Strother, R. Hamers, and L. Smith, Nucleic Acids Res. **28**, 3535 (2000).
[17]A. Pike, L. Lie, R. Eagling, L. Ryder, S. Patole, B. Connolly, B. R. Horrocks, and A. Houlton, Angew. Chem., Int. Ed. **41**, 615 (2002).
[18]L. Lie, S. Patole, A. Pike, L. Ryder, B. Connolly, A. Ward, E. Tuite, A. Houlton, and B. R. Horrocks, Faraday Discuss. **125**, 235 (2004).
[19]G. Francia, V. Ferrara, S. Manzo, and S. Chiavarini, Biosens. Bioelectron. **21**, 661 (2005).
[20]G. Demirel, Z. Rzaev, S. Patir, and E. Piskin, J. Nanosci. Nanotechnol. **9**, 1865 (2009).
[21]Z. Li, Y. Chen, X. Kamins, T. Nauka, and R. Williams, Nano Lett. **4**, 245 (2004).
[22]L. Wang, V. Reipa, and J. Blasic, Bioconjugate Chem. **15**, 409 (2004).
[23]L. Lie, M. Duerdin, E. Tuite, A. Houlton, and B. R. Horrocks,. J. Electroanal. Chem., **538–539**, 183 (2002).
[24]Y. Chao, S. Krishnamurthy, M. Montalti, L. Lie, A. Houlton, B. R. Horrocks, L. Kjeldgaard, V. Dhanak, M.R.C. Hunt, and L. Šiller, J. Appl. Phys. **98**, 044316 (2005).
[25]Y. Chao, A. Houlton, B. R. Horrocks, M. R. C. Hunt, N. R. J. Poolton, J. Yang, and L. Šiller, Appl. Phys. Lett. **88**, 263119 (2006).
[26]Y. Chao, L. Šiller, S. Krishnamurthy, P. R. Coxon, U. Bangert, M. Gass, L. Kjeldgaard, S. N. Patole, L. H. Lie, N. O'Farrell, T. A. Alsop, A. Houlton, and B. R. Horrocks, Nat. Nanotechnol. **2**, 486 (2007).
[27]L. Šiller, S. Krishnamurthy, L. Kjeldgaard, B. R. Horrocks, Y. Chao, A. Houlton, A. Chakraborty, and M. R. C. Hunt,. J. Phys.: Condens. Matter **21**, 095005 (2009).
[28]N. H. Al-Sharif, C. E. M. Berger, S. S. Varanasi, Y. Chao, B. R. Horrocks, and H. K. Datta Small **5**, 221 (2009).
[29]Y. Wang, J. Zheng, Z. Zhang, C. Yuan, and D. Fu, Colloids Surf., A **342**, 102 (2009).
[30]A. Rogalev and J. Goulon, in *Chemical Applications of Synchrotron Radiation*, edited by T. Sham (World Scientific, Singapore, 2002), Chap. 15, p. 707.
[31]F. Quinn, N. Poolton, A. Malins, E. Pantos, C. Andersen, P. Denby, and V. Dhanak, J. Synchrotron Radiat. **10**, 461 (2003).
[32]T. Sham, R. Sammynaiken, Y. Zhu, P. Zhang, I. Coulthard, and S. Naftel, Thin Solid Films **363**, 318 (2000).
[33]P. Batson and J. Heath, Phys. Rev. Lett. **71**, 911 (1993).
[34]Corrigendum on M. Rosso Vasic, E. Spruijt, B. Lagen, L. de Cola, and H. Zuilhof, Small **4**, 1835 (2008).
[35]T. Sham, S. Naftel, P. Kim, R. Sammynaiken, Y. Tang, I. Coulthard, A. Moewes, J. Freeland, Y. Hu, and S. Lee, Phys. Rev. B **70**, 045313 (2004).
[36]S. Rath, G. Chainy, S. Nozaki, and S. Sahu, Physica E **30**, 182 (2005).

[37]S. Rath, G. Chainy, S. Nozaki, and S. Sahu, Nanotechnology **19**, 115606 (2008).
[38]S. Flock, R. Labarbe, and C. Houssier, Biophys. J. **70**, 1456 (1996).
[39]H. Yoo and P. Fauchet, Proc. Soc. Photo-Opt. Instrum. Eng. **6902**, 690203 (2008).
[40]J. Riegler, F. Ditengou, K. Palme, and T. Nann, J. Nanobiotechnol. **6**, 10803 (2008).
[41]J. Stöhr, *NEXAFS Spectroscopy*, 2nd ed. (Springer-Verlag, Berlin, 2003).
[42]Y. Zubavichus, A. Shaporenko, M. Grunze, and M. Zharnikov, J. Phys. Chem. A **109**, 6998 (2005).
[43]T. Sham, in *Topics in Current Chemistry: Synchrotron Radiation in Chemistry and Biology I*, edited by E. Mandelkow (Springer-Verlag, Berlin, 1988), Chap. 4, p. 81.
[44]P. Leinweber, J. Kruse, F. Walley, A. Gillespie, K. Eckhardt, R. Blyth, and T. Reiger, J. Synchrotron Radiat. **14**, 500 (2007).
[45]Y. Zubavichus, A. Shaporenko, V. Korolkov, M. Grunze, and M. Zharnikov, J. Phys. Chem. B **112**, 13711 (2008).
[46]X. Liu, F. Zheng, A. Jurgensen, V. Perez-Dieste, D. Petrovykh, N. Abbott, and F. Himpsel, Can. J. Chem. **85**, 793 (2007).
[47]A. Moewes, J. MacNaughton, R. Wilks, J. Lee, S. Wettig, H. Kraatz, and E. Kurmaev,. J. Electron Spectrosc. **137–140**, 817 (2004).
[48]E. Buzaneva, A. Gorchynskyy, G. Popova, A. Karlash, Y. Shtogun, K. Yakovkin, D. Zherebetsky, O. Matyshevska, Y. Prylutskyy, and P. Scharff, in *Frontiers of Multifunctional Nanosystems*, edited by E. Buzaneva and P. Scharff (Kluwer Academic Publishers, Dordrecht, 2002), Vol. **191**.
[49]J. Crain, A. Kirakosian, J. Lin, Y. Gu, R. Shah, N. Abbott, and F. Himpsel, J. Appl. Phys. **90**, 8979 (2001).
[50]C. Lee, L. Gamble, D. Grainger, and D. Castner, Biointerphases **1**, 82 (2006).
[51]K. Fujii, K. Akamatsu, Y. Muramatsu, and A. Yokoya, Nucl. Instrum. Methods Phys. Res. B **199**, 249 (2003).
[52]Y. Harada, T. Takeuchi, H. Kino, A. Fukushima, K. Takakura, K. Hieda, A. Nakao, S. Shin and H. Fukuyama, J. Phys. Chem. A **110**, 13227 (2006).
[53]O. Plekan, V. Feyer, R. Richter, M. Coreno, M. de Simone, K. Prince, A. Trofimov, E. Gromov, I. Zaytseva, and J. Schirmer, Chem. Phys. **347**, 360 (2008).
[54]S. Seifert, G. Gavrila, D. Zahn, and W. Braun, Surf. Sci. **601**, 2291 (2007).
[55]N. Samuel, C. Lee, L. Gamble, D. Fischer, and D. Castner, J. Electron Spectrosc. **152**, 134 (2006).
[56]S. Ptasinska, A. Stypczynska, T. Nixon, N. J. Mason, D. V. Klyachko, and L. Sanche, J. Chem. Phys. **129**, 065102 (2008).
[57]B. Boudaiffa, P. Cloutier, D. Hunting, M. A. Huels, and L. Sanche, Science **287**, 1658 (2000).
[58]N. O'Farrell, A. Houlton, and B. Horrocks, Int. J. Nanomed. **1**, 451 (2006).
[59]See supplementary material at http://dx.doi.org/10.1063/1.3691600 for details of preparation, FTIR, XAS and Raman characterization, particle size determination and molecular models.